

# Electronic Supporting Information

## High-efficiency Solution-processed Light-emitting Diode Based on a Phosphorescent Ag<sub>3</sub>Cu<sub>5</sub> Cluster Complex

Zhu Jiao,<sup>ab</sup> Ming Yang,<sup>\*b</sup> Jin-Yun Wang,<sup>b</sup> Ya-Zi Huang,<sup>b</sup> Pei Xie,<sup>a,b</sup> Zhong-Ning Chen<sup>\*abc</sup>

<sup>a</sup> College of Chemical Engineering, Fuzhou University, Fuzhou, Fujian 350108, China

<sup>b</sup> State Key Laboratory of Structural Chemistry, Fujian Institute of Research on the Structure of Matter, Chinese Academy of Sciences, Fuzhou, Fujian 350002, China. Email: [czn@fjirsm.ac.cn](mailto:czn@fjirsm.ac.cn), [ym31023@fjirsm.ac.cn](mailto:ym31023@fjirsm.ac.cn)

<sup>c</sup> Fujian Science & Technology Innovation Laboratory for Optoelectronic Information of China, Fuzhou, Fujian 350108, China

**Table S1.** Crystal Data and Structure Refinement for Ag<sub>3</sub>Cu<sub>5</sub> Cluster Complex.

	Ag <sub>3</sub> Cu <sub>5</sub> Cluster
chemical formula	C <sub>255</sub> H <sub>239</sub> N <sub>9</sub> P <sub>6</sub> Ag <sub>3</sub> Cu <sub>5</sub> Cl <sub>2</sub> O <sub>8</sub>
formula weight	4455.57
crystal system	Triclinic
space group	$P \bar{1}$
$T$ (k)	273 (2)
$a$ (Å)	15.479 (2)
$b$ (Å)	15.967 (2)
$c$ (Å)	54.448 (6)
$\alpha$ (°)	83.158 (5)
$\beta$ (°)	89.009 (4)
$\gamma$ (°)	75.683 (6)
$V$ (Å <sup>3</sup> )	12943.32 (3)
$Z$	2
density (g/cm <sup>3</sup> )	1.143
reflns collected	196725
unique reflns	47348
$R_{\text{int}}$	0.171
$F(000)$	4612
$R_1^a$ [ $I > 2\sigma(I)$ ]	0.082
$wR_2^b$ [ $I > 2\sigma(I)$ ]	0.261
GOF	1.01

<sup>a</sup> $R_1 = \Sigma||F_o| - |F_c|| / \Sigma|F_o|$ ,    <sup>b</sup> $wR_2 = [\Sigma w(|F_o| - |F_c|)^2 / \Sigma w|F_o|^2]^{1/2}$ .

**Table S2.** Selected Interatomic Distances (Å) and Bond Angles (°) of Ag<sub>3</sub>Cu<sub>5</sub> Cluster Complex.

Ag1–Cu1	2.6379(10)	Ag1–Cu2	2.6529(11)
Ag2–Cu1	2.6616(11)	Ag2–Cu3	2.6485(10)
Ag3–Cu2	2.6702(11)	Ag3–Cu3	2.6818(9)
Cu1–Cu4	2.5555(12)	Cu1–Cu5	2.5928(12)
Cu2–Cu4	2.6269(11)	Cu2–Cu5	2.5346(11)
Cu3–Cu4	2.5248(13)	Cu5–Cu3	2.5956(13)
Cu4–Cu5	2.6979(12)	Ag1–C143	2.549(7)
Ag1–P6	2.490(2)	Ag1–P1	2.5038(19)
Ag2–C171	2.510(7)	Ag3–C115	2.450(8)
Ag2–P4	2.476(2)	Ag2–P5	2.467(2)
Ag3–P2	2.4709(18)	Ag3–P3	2.447(2)
Cu1–C89	1.952(8)	Cu1–C199	1.947(8)
Cu1–N3	2.057(6)	Cu2–N1	2.063(5)
Cu2–C115	1.958(8)	Cu2–C143	1.960(8)
Cu3–C171	1.976(7)	Cu3–C227	1.962(7)
Cu3–N2	2.073(6)	Cu4–C89	2.063(8)
Cu4–C115	2.094(7)	Cu4–C171	2.074(7)
Cu5–C143	2.083(7)	Cu5–C199	2.040(7)
Cu5–C227	2.073(8)		
P6–Ag1–P1	118.04(7)	P1–Ag1–C143	92.93(16)
P6–Ag1–C143	123.28(18)	P6–Ag1–C89	89.51(17)
P1–Ag1–C89	116.81(16)	C143–Ag1–C89	118.8(2)
P5–Ag2–P4	119.78(6)	P5–Ag2–C171	118.00(18)
P4–Ag2–C171	93.50(18)	P5–Ag2–C199	91.12(17)
P4–Ag2–C199	120.80(19)	C171–Ag2–C199	116.0(2)
P3–Ag3–C115	119.0(2)	P3–Ag3–P2	120.03(7)
C115–Ag3–P2	93.05(16)	P3–Ag3–C227	93.95(18)
C115–Ag3–C227	112.7(2)	P2–Ag3–C227	120.04(18)
C199–Cu1–C89	161.3(3)	C199–Cu1–N3	98.6(3)
C89–Cu1–N3	100.0(3)	C115–Cu2–N1	97.6(3)
C115–Cu2–C143	160.9(3)	C143–Cu2–N1	101.4(3)
C227–Cu3–C171	161.1(3)	C227–Cu3–N2	97.3(3)
C171–Cu3–N2	101.4(3)	C89–Cu4–C171	111.8(3)
C89–Cu4–C115	121.5(3)	C171–Cu4–C115	115.5(3)
C199–Cu5–C227	120.1(3)	C199–Cu5–C143	114.0(3)
C227–Cu5–C143	113.2(3)		

**Table S3.** The Partial Molecular Orbital Compositions (%) by SCPA Approach and the Absorption Transitions in the Ground State for Ag<sub>3</sub>Cu<sub>5</sub> Cluster Complex in the CH<sub>2</sub>Cl<sub>2</sub> Solution Calculated by TD-DFT Method at the PBE1PBE Level

orbital	energy (eV)	MO contribution (%)			
		Cu (s/p/d)	Ag (s/p/d)	dpppy	ebzcz
LUMO+8	-1.53	47.98 (86/13/1)	22.05 (81/10/9)	19.36	10.61
LUMO+7	-1.56	43.43 (67/30/3)	33.69 (85/10/5)	20.66	2.21
LUMO+1	-1.83	22.42 (39/56/5)	43.13 (88/9/3)	19.15	15.30
LUMO	-1.94	21.01 (23/72/5)	46.82 (85/12/3)	13.97	18.20
HOMO	-5.47	35.42 (14/7/79)	7.06 (72/6/22)	6.78	50.75
HOMO-1	-5.52	32.74 (13/5/82)	4.27 (54/8/38)	8.12	54.87
HOMO-2	-5.62	13.27 (35/11/54)	3.69 (58/12/29)	1.18	81.86
HOMO-3	-5.71	9.54 (47/13/40)	6.70 (69/17/14)	1.58	82.18
HOMO-6	-5.87	34.05 (6/4/89)	4.04 (36/17/47)	7.51	54.41

state	<i>E</i> , nm (eV)	O.S.	transition (contrib.)	assignment	measured (nm)
S <sub>1</sub>	444 (2.79)	0.0730	HOMO→LUMO (67%)	<sup>1</sup> MC/ <sup>1</sup> LMCT/ <sup>1</sup> IL	435
			HOMO-1→LUMO (11%)	<sup>1</sup> MC/ <sup>1</sup> LMCT/ <sup>1</sup> IL	
S <sub>2</sub>	436 (2.85)	0.0526	HOMO-1→LUMO (48%)	<sup>1</sup> MC/ <sup>1</sup> LMCT/ <sup>1</sup> IL	
			HOMO-6→LUMO (12%)	<sup>1</sup> MC/ <sup>1</sup> LMCT/ <sup>1</sup> IL	
S <sub>3</sub>	432 (2.87)	0.0664	HOMO→LUMO+1 (53%)	<sup>1</sup> MC/ <sup>1</sup> LMCT/ <sup>1</sup> IL/ <sup>1</sup> LLCT	
			HOMO-1→LUMO+1 (13%)	<sup>1</sup> MC/ <sup>1</sup> LMCT/ <sup>1</sup> IL/ <sup>1</sup> LLCT	
S <sub>16</sub>	381 (3.25)	0.9183	HOMO-2→LUMO+1 (18%)	<sup>1</sup> LMCT/ <sup>1</sup> LLCT/ <sup>1</sup> IL/ <sup>1</sup> MC	368
			HOMO-3→LUMO (17%)	<sup>1</sup> LMCT/ <sup>1</sup> IL/ <sup>1</sup> LLCT	
S <sub>26</sub>	363 (3.41)	0.3998	HOMO-1→LUMO+8 (19%)	<sup>1</sup> MC/ <sup>1</sup> LMCT/ <sup>1</sup> LLCT/ <sup>1</sup> IL	350
			HOMO→LUMO+7 (14%)	<sup>1</sup> MC/ <sup>1</sup> LMCT/ <sup>1</sup> LLCT	

**Table S4.** The Partial Molecular Orbital Compositions (%) by SCPA Approach and Emission Transitions in the Lowest-Energy Triplet State for Ag<sub>3</sub>Cu<sub>5</sub> Cluster Complex in the CH<sub>2</sub>Cl<sub>2</sub> Solution Calculated by TD-DFT Method at the PBE1PBE Level.

orbital	energy (eV)	MO Contribution (%)			
		Cu (s/p/d)	Ag (s/p/d)	dpppy	ebzcz
LUMO	-2.30	20.83 (25/67/8)	19.31 (77/12/11)	53.52	6.34
HOMO	-5.38	38.84 (16/6/78)	5.70 (70/6/24)	8.55	46.90

state	<i>E</i> , nm (eV)	O.S.	transition (contrib.)	assignment	measured (nm)
T <sub>1</sub>	592 (2.09)	0.0000	HOMO->LUMO (74%)	<sup>3</sup> LLCT/ <sup>3</sup> MC	590

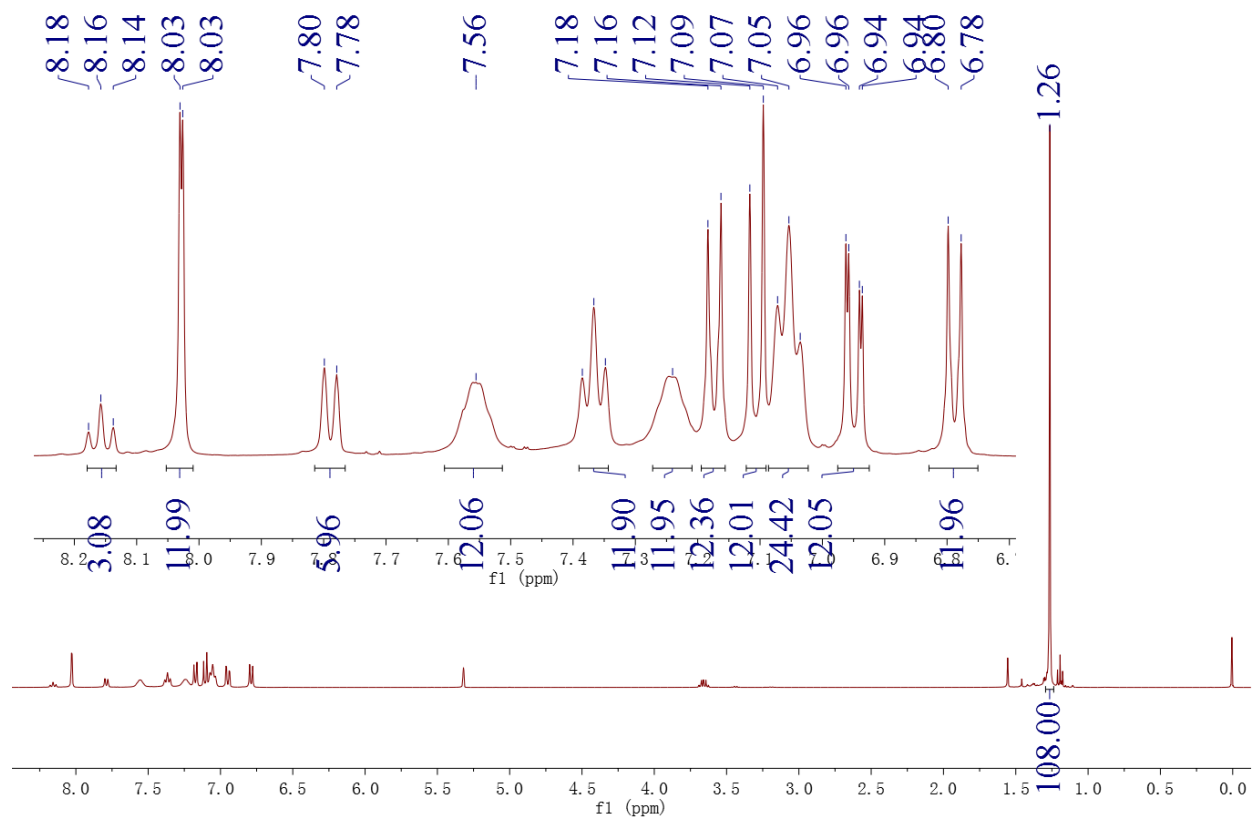


**Fig. S1** The  $^1\text{H}$  NMR spectrum of  $\text{Ag}_3\text{Cu}_5$  cluster compound in  $\text{CD}_2\text{Cl}_2$  solution at ambient temperature.

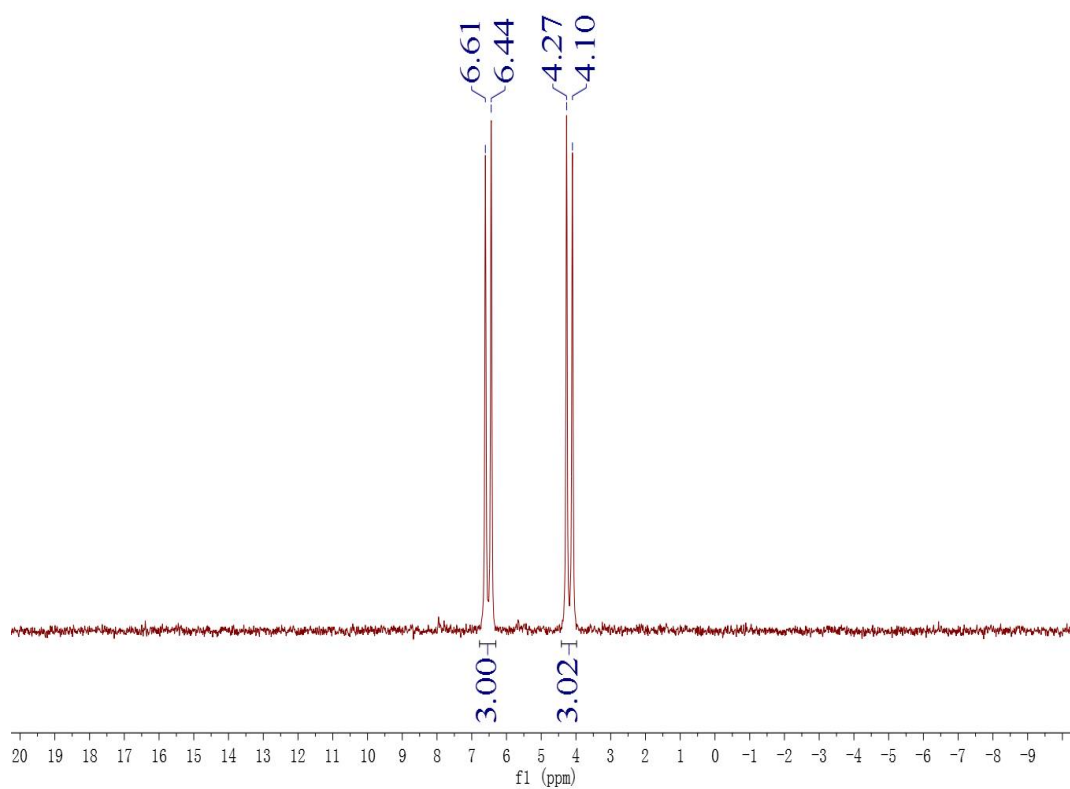


**Fig. S2** The  $^{31}\text{P}$  NMR spectrum of  $\text{Ag}_3\text{Cu}_5$  cluster compound in  $\text{CD}_2\text{Cl}_2$  solution at ambient temperature.

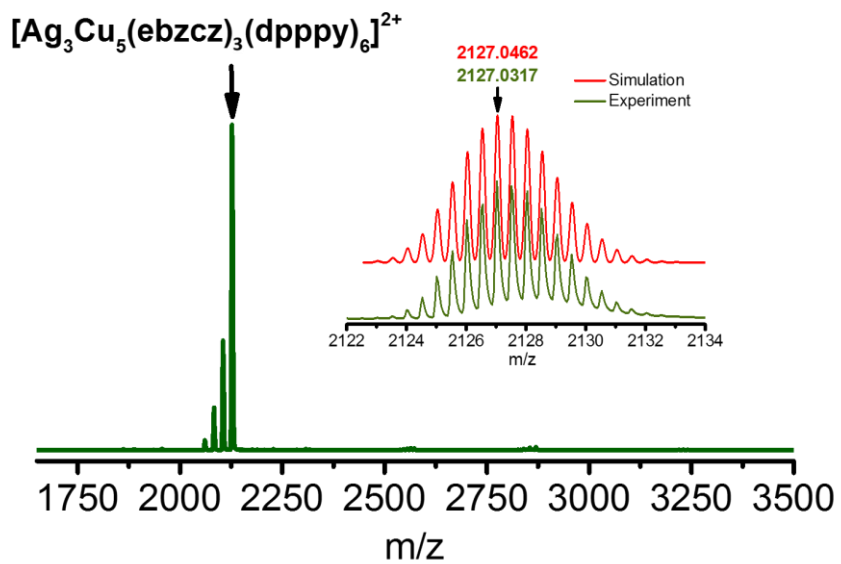


**Fig. S3** The high-resolution mass spectrometry of  $\text{Ag}_3\text{Cu}_5$  cluster compound. Inset: The measured (green) and simulated (red) isotopic patterns.

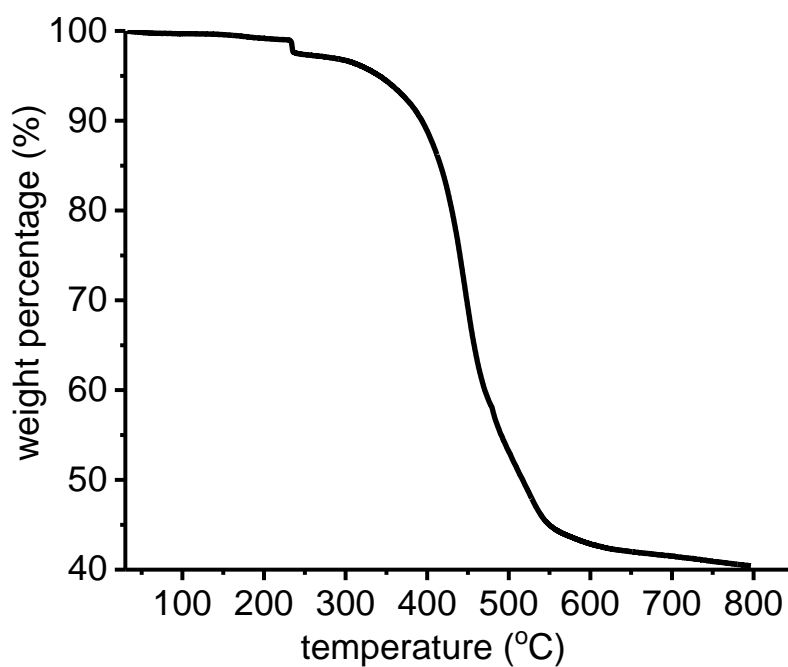


**Fig. S4** The plot of thermogravimetric analysis of  $\text{Ag}_3\text{Cu}_5$  cluster compound.

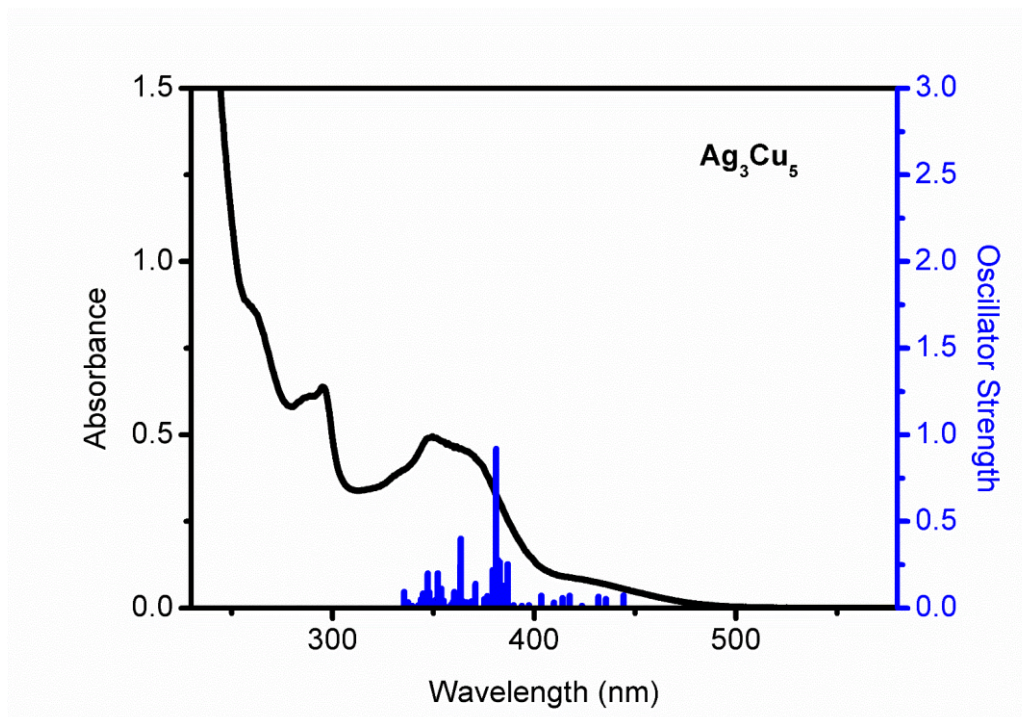


**Fig. S5** The calculated (blue bars) and experimentally measured (black line) absorption spectra of  $\text{Ag}_3\text{Cu}_5$  cluster compound in  $\text{CH}_2\text{Cl}_2$  solution at ambient temperature, calculated by TD-DFT method at the PBE1PBE level.

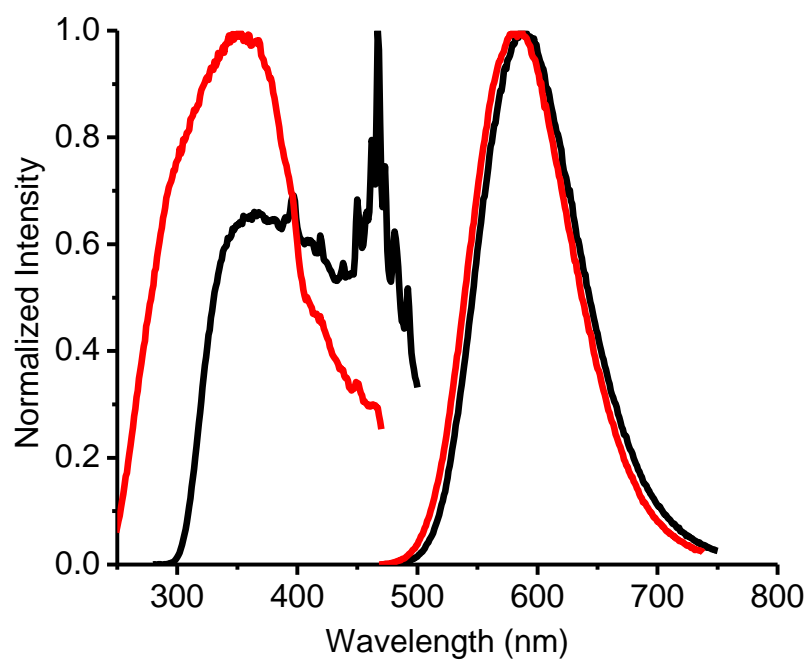


**Fig. S6** The excitation and emission spectra of  $\text{Ag}_3\text{Cu}_5$  cluster compound in solid state (black) and film (red) at room temperature.

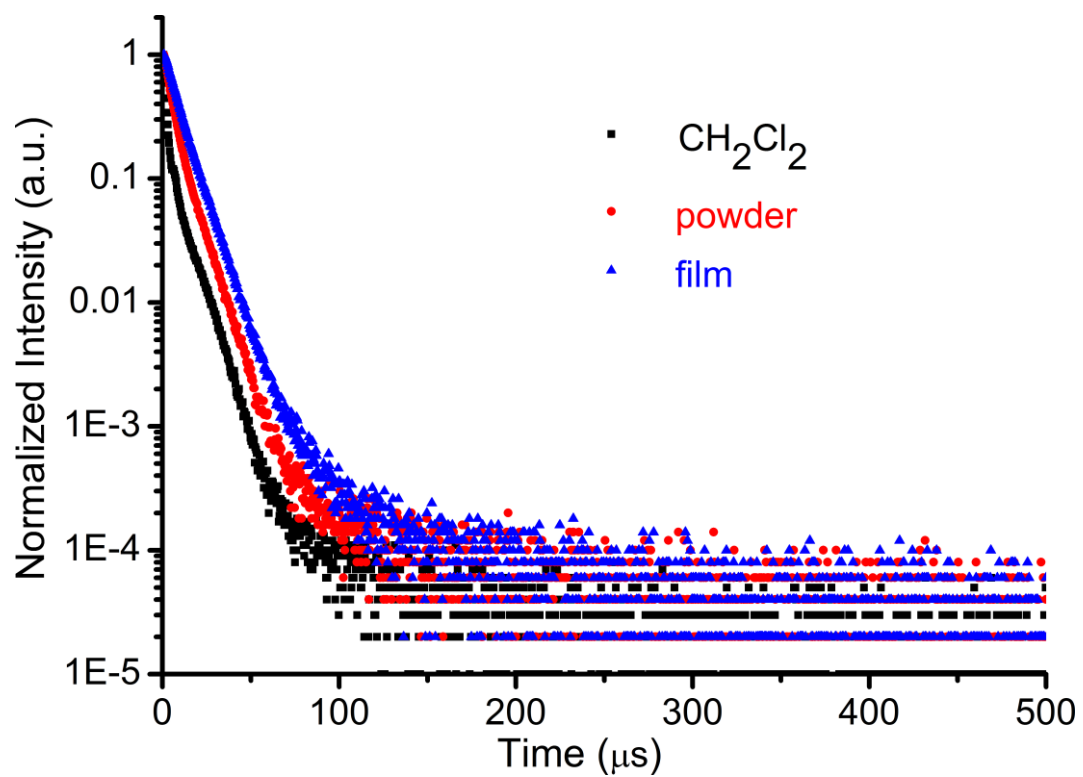


**Fig. S7** The luminescent decay curves of  $\text{Ag}_3\text{Cu}_5$  cluster compound in  $\text{CH}_2\text{Cl}_2$ , powder and film states at room temperature.



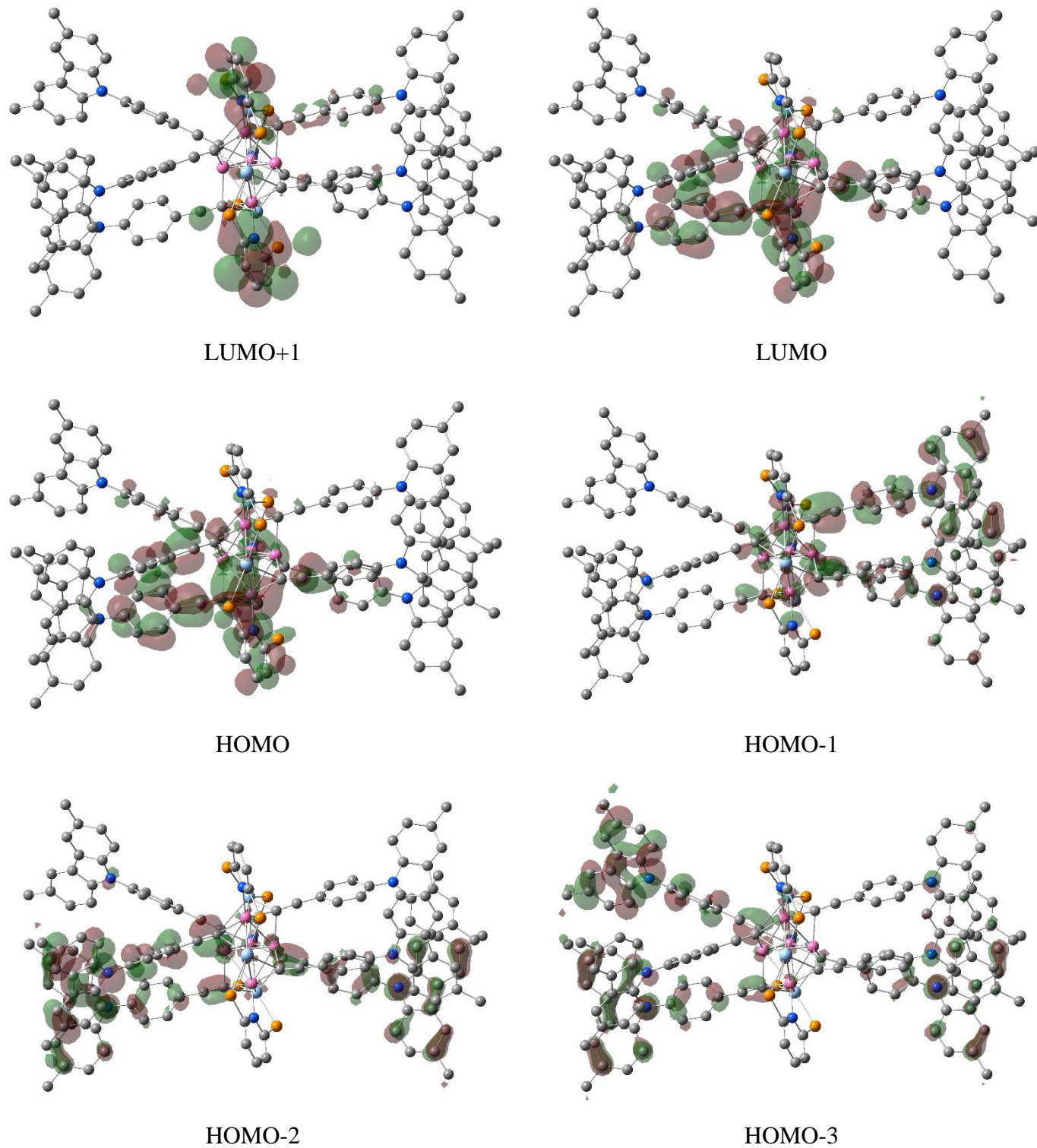


**Fig. S8** Plots of the frontier molecular orbitals involved in the absorption transition (isovalue = 0.02) for  $\text{Ag}_3\text{Cu}_5$  cluster compound by TD-DFT method at the PBE1PBE level.